Progress In Electromagnetics Research Letters, Vol. 58, 9–16, 2016

Design of Compact Microstrip UWB Bandpass Filter with Triple-Notched Bands

Chengpei Tang* **and Nian Yang**

Abstract—A new microstrip ultra-wideband (UWB) bandpass filter (BPF) with triple-notched bands is presented in this paper. The circuit topology and its corresponding electrical parameters of the basic microstrip UWB BPF are designed by modified genetic algorithm (MGA). Then, triple-notched bands inside the UWB passband are implemented by coupling a novel triple-mode stepped impedance resonator (SIR) to the main transmission line of the basic microstrip UWB BPF. The triple-notched bands can be easily generated and set at any desired frequencies by varying the designed parameters of triple-mode SIR. For verification, a new microstrip UWB BPF with triple-notched bands respectively centered at frequencies of 4.4 GHz, 5.9 GHz and 8.0 GHz is designed and fabricated. Both simulated and experimental results are provided with good agreement.

1. INTRODUCTION

In February 2002, the U.S. Federal Communications Commission allocated 3.1–10.6 GHz band as unlicensed spectrum for ultra-wideband (UWB) systems [1]. A UWB BPF, as one of the essential components of the UWB systems, has gained much attention in recent years. There are many techniques presented to design UWB bandpass filters. For example, multiple-mode resonator (MMR) [2, 3], multilayer coupled structure [4, 5], defected ground structure (DGS) [5, 6], defected microstrip structure (DMS) [7], and the cascaded low-pass/high-pass filters [8] have been widely used to achieve UWB characteristics.

However, the existing wireless networks such as 4.5G satellite communication systems signals, 5.8 GHz WLAN signals, and some 8.0 GHz satellite communication systems signals can easily interfere with UWB users. Therefore, compact UWB BPF with multiple notched bands is emergently required to reject these interfering signals [9–15]. To achieve a notched band, one of two arms in the coupled-line sections is extended and folded in [9]. On the other side, the coupling interdigital line is introduced to block undesired existing radio signals in [10]. However, these two methods can only achieve one notched band. Thus, to introduce dual-notched bands, a coupled simplified composite right/left-handed resonator is introduced in [11], and two coupled stepped impedance resonators are employed in [12]. However, the selectivity designed with these two methods need to be improved. By arranging two asymmetric meander open-loop resonators on middle layer and a C-shaped resonator on bottom layer [13] or embedding two open-circuit stubs into broadside-coupled stepped impedance resonators on middle layer [14], dual-notched bands can be introduced into an UWB BPF. Additionally, by integrating short-circuited stub resonators [15] or embedding a quarter-wavelength coplanar waveguide resonators and inserting a meander slot-line in the detached-mode resonator [16] can also realize dual-notched bands. However, these designs are based on multilayer technology which will increase the fabrication cost. A new method based on wave's cancellation theory has been proposed to design an UWB BPF with dual-notched band in [17]. However, the center frequencies and bandwidths of the notched bands cannot be

Received 29 July 2015, Accepted 22 September 2015, Scheduled 7 December 2015
* Corresponding author: Chengpei Tang (tchengp@mail.sysu.edu.cn).
The authors are with the School of Engineering, Sun Yat-sen University, Guangzhou 510006, China.

adjusted. Two tri-section stepped impedance resonators and a parallel gap-coupled microstrip resonator are used in [18], and two L-shaped folded shunt open-circuited stubs are placed on the feed lines in [19] to achieve triple-notched bands. However, the performance of the filter is not ideal. Furthermore, design efficiencies of the filters mentioned above need to be improved.

In this paper, we present a new UWB BPF with triple-notched bands. The basic microstrip UWB BPF is designed by modified genetic algorithm (MGA) to simultaneously search for the appropriate circuit topology and its corresponding electrical parameters. By improving the fitness evaluation, selection, crossover, and mutation, we overcome two possible drawbacks of conventional GA, i.e., slow rate of convergence and local-best solution, thus to achieve better accuracy and high efficiency for UWB BPF design. Then, triple-notched bands property is achieved by coupling a novel triple-mode stepped impedance resonator (SIR) to the main transmission line. The triple-notched bands can be easily generated and realized by controlling the locations of even-odd modes resonance frequency of the triple-mode stepped SIR. Finally, the proposed filter is designed, fabricated and measured. Good agreement between measured and simulated results is achieved.

2. UWB BANDPASS FILTER DESIGN

An arbitrary two-port microstrip circuit shown in Fig. 1(a) can be decomposed into basic circuit elements [20, 21] shown in Fig. 1(b). The circuit can be expressed as a data structure shown in Fig. 1(c). The data structure is composed of three parts. The first part coded in integer represents the topology of basic element. The second part coded in integer represents the way of connection to the previous element. The third part coded in floating number represents the corresponding electrical parameters. In the GA, we define a basic circuit element as a gene and a set of basic circuit elements as a chromosome. Therefore, an arbitrary two-port circuit can be represented by a chromosome. Table 1 is the details of the basic circuit elements. A special gene named *Empty* is introduced, which enables the representation scheme to describe a circuit with an arbitrary number of basic circuit elements and orders. In this work, we adopt the MGA to design a microstrip UWB BPF with improved design efficiency.

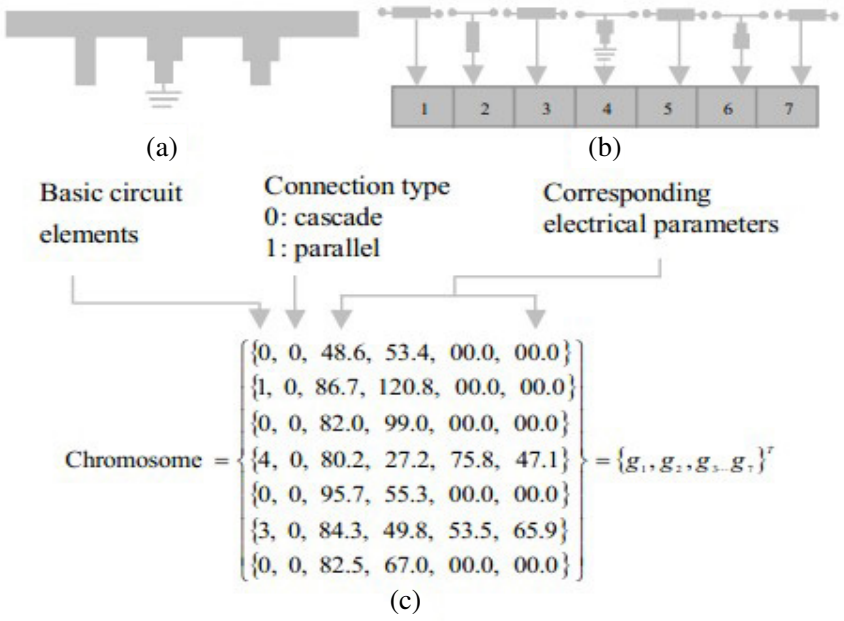

Figure 1. Representation scheme in the modified genetic algorithm: (a) a typical microstrip circuit, (b) decomposition of the circuit in (a) into basic circuit elements, (c) chromosome of the circuit in (a).

Table 1. Details of the basic elements in the modified genetic algorithm.

Category	Type	Name	Network Topology	Electrical Parameters
Basic Circuit Elements	0	TL		Z_{01} θ_{01}
	1	Open		Z_{01} θ_{01}
	2	Short		Z_{01} θ_{01}
	3	SIR_Open		Z_{01} θ_{01} Z_{02} θ_{02}
	4	SIR_Short		Z_{01} θ_{01} Z_{02} θ_{02}
	5	Empty		0 0 0 0

2.1. Initialization

Because the initial population affects convergence, we make each chromosome randomly initialized within the specific electrical parameters' range for each basic element. In addition, it is necessary to assign upper and lower limits according to various designs and engineering requirements. Due to the tolerance of the fabrication, the minimum width is limited to 0.1 mm, which corresponds to a microstrip line with a characteristic impedance of 137 Ω. Meanwhile, to lower the junction discontinuity effects, the maximum line width is chosen to be 2 mm, which corresponds to a microstrip line with a characteristic impedance of 40 Ω.

2.2. Fitness Evaluation

The transmission-line models are used to calculate scattering parameters to effectively evaluate the frequency response of a chromosome. We make $ABCD$ matrix multiplication as cascade no matter the basic element is in series or parallel connection. It should be mentioned that the gene named *Empty* represents unit matrix. The method will improve the calculation speed of procedures and efficiency of algorithm. The desired function is shown in Fig. 2, and the fitness value is defined by:

$$F = \sum_{i=1}^{N} w_i f_i \tag{1}$$

where w_i represents the weighting value at the ith sampling point, f_i the square deviation between the calculated scattering parameter and the desired value at the ith sampling point, and N the number of sampling points.

2.3. Genetic Operator

Although the roulette wheel selection based on the proportionate selection is widely used in the GA, there is a drawback that the type of fitness function has an effect on the convergence. Thus, in this paper, the tournament selection is used.

Crossover operator is an important operator and plays a decisive role in global convergence of the algorithm. The way of the crossover decides whether we can find the optimal solution and the speed of finding the optimal solution. Therefore, the scheme employs a high efficiency crossover method of combining bubble sort with single-point crossover.

Mutation as a reproduction operator has a key role of getting out from the trap of the local optimum solution and keeping the diversity of population. In this work, mutation is carried out to randomly alter the values of genes in a parent chromosome with probability.

2.4. Result and Performance

Here, an initial microstrip UWB BPF is designed by the MGA. For the design, the best chromosome after 18 generations consists of four empty elements, five transmission lines, and four stubs. The proposed filter is realized on the substrate Duroid 5880 ($\varepsilon_r = 3.38$, $h = 0.508$, $\tan\delta = 0.003$). Table 2 lists the electrical and final physical parameters. Notice that we have slightly adjusted some initial physical parameters considering the discontinuity effects and fringing capacitances. The simulated scattering parameters are shown in Fig. 3. Referring to Fig. 3, the proposed UWB BPF has an insertion loss better than 3 dB over the 3.34–11.08 GHz bandwidth, and the upper-stopband with −10 dB attenuation is up to 15 GHz.

3. TRIPLE-MODE SIR ANALYSIS

To realize band-notched characteristics, we introduce a novel triple-mode SIR into the basic UWB BPF. This structure is simple and flexible for blocking undesired narrow band radio signals that may appear in UWB band. The proposed triple-mode SIR is composed of a stepped impedance hairpin resonator

Table 2. Electrical and physical parameters of the basic UWB BPF.

No.	Name	Electrical Parameters (at $f_0 = 6.9$ GHz)				Physical Parameters in mm			
		z_{01}	θ_{01}	z_{02}	θ_{02}	W_{01}	L_{01}	W_{02}	L_{02}
1	Short	97.8	70.3	0	0	0.3	5.4	0	0
2	TL	52.2	47.8	0	0	1.1	3.5	0	0
3	Empty	0	0	0	0	0	0	0	0
4	TL	72.7	66.7	0	0	0.6	5	0	0
5	TL	67.3	71.0	0	0	0.7	5.3	0	0
6	Empty	0	0	0	0	0	0	0	0
7	SIR_Short	52.2	66.9	67.3	21.4	1.1	4.9	0.7	1.6
8	TL	58.6	74.3	0	0	0.9	5.5	0	0
9	Empty	0	0	0	0	0	0	0	0
10	Open	72.7	20.6	0	0	0.6	1.5	0	0
11	Empty	0	0	0	0	0	0	0	0
12	TL	72.9	37.3	0	0	0.6	2.8	0	0
13	SIR_Short	87.3	84.0	67.3	20.1	0.4	6.4	0.7	1.5

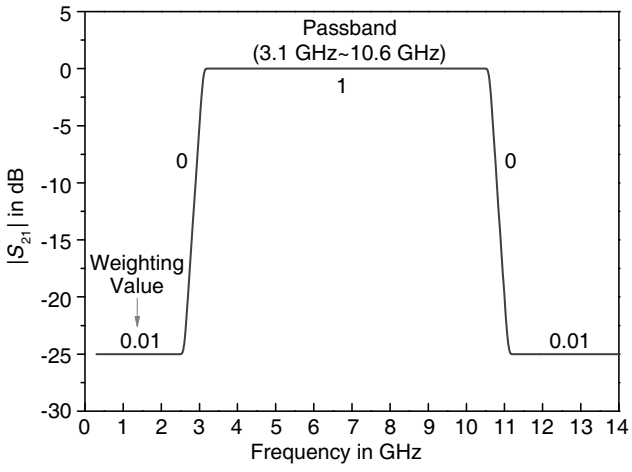

Figure 2. The desired function of the proposed basic UWB BPF.

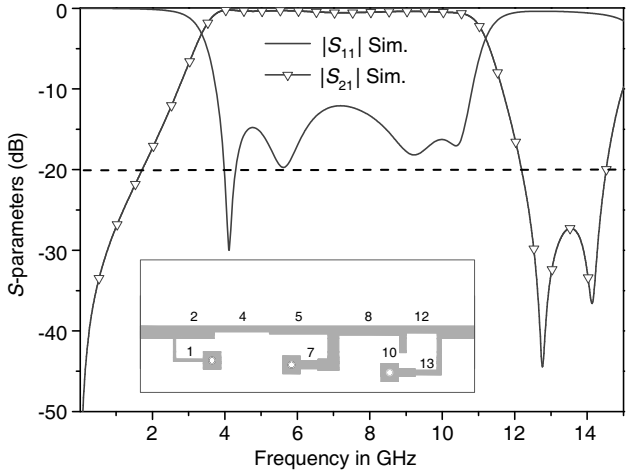

Figure 3. Simulated performance of proposed basic UWB BPF.

and two short-ended stubs. Fig. 4 shows the layout of the E-shaped resonator coupled to a section of main transmission line and its corresponding equivalent circuit. Since the resonator is symmetrical to the A-A' and B-B' plane, the resonance properties of the triple-mode SIR can be analyzed by the even-odd modes analysis method. Under mode excitation, the resonator electrical field distribution of the resonator exhibits either an even or an odd mode distribution property as shown in Fig. 5. For the even mode condition, the electrical fields exhibit a symmetric distribution along the B-B' axis as shown in Fig. 5(a). On the other hand, for the odd mode, the electrical fields exhibit an anti-symmetric distribution along the A-A' axis as shown in Fig. 5(b) and the B-B' axis as shown in Fig. 5(c). Thus, based on the electrical field distribution property, the even-odd modes resonance frequencies can be deduced as:

$$f_{\text{notch}} = \frac{c}{\lambda_{\text{notch}}\sqrt{\varepsilon_{eff}}} \tag{2}$$

$$f_{\text{notch-even1}} = \frac{c}{4(L_{e2}+L_{e3}+L_{e4})\sqrt{\varepsilon_{eff}}} \tag{3}$$

$$f_{\text{notch-odd1}} = \frac{c}{2(L_{e1}+2L_{e2}+L_{e4})\sqrt{\varepsilon_{eff}}} \tag{4}$$

$$f_{\text{notch-odd2}} = \frac{c}{4(L_{e2}+L_{e4})\sqrt{\varepsilon_{eff}}} \tag{5}$$

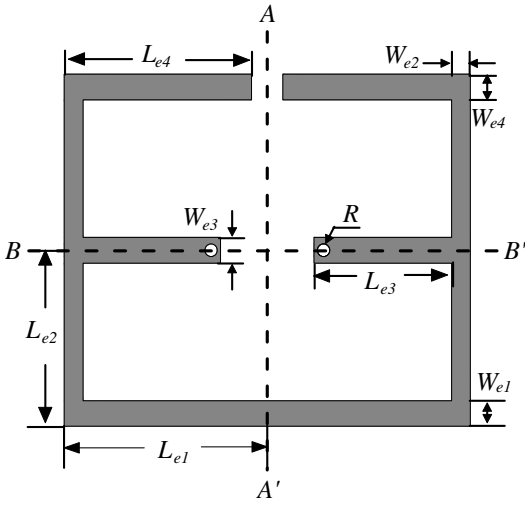

Figure 4. Geometry of the proposed triple-mode SIR.

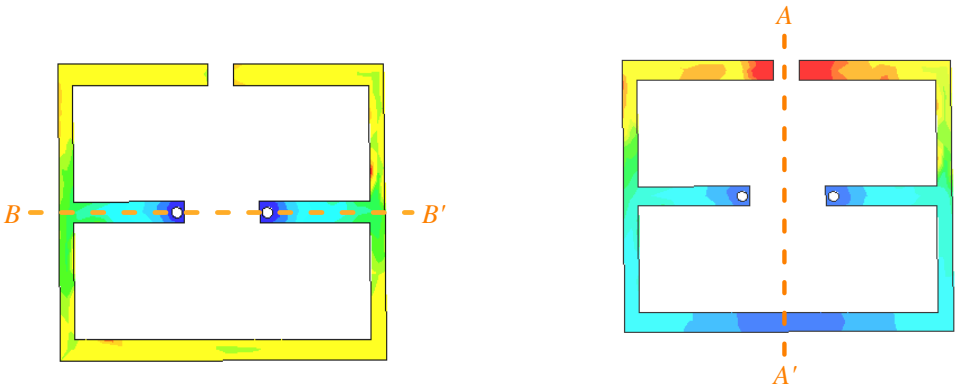

(a) (b)

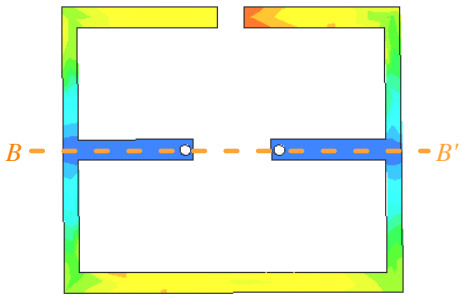

(c)

Figure 5. Electrical field distribution of the proposed triple-mode SIR: (a) even mode, (b) odd mode, (c) odd mode.

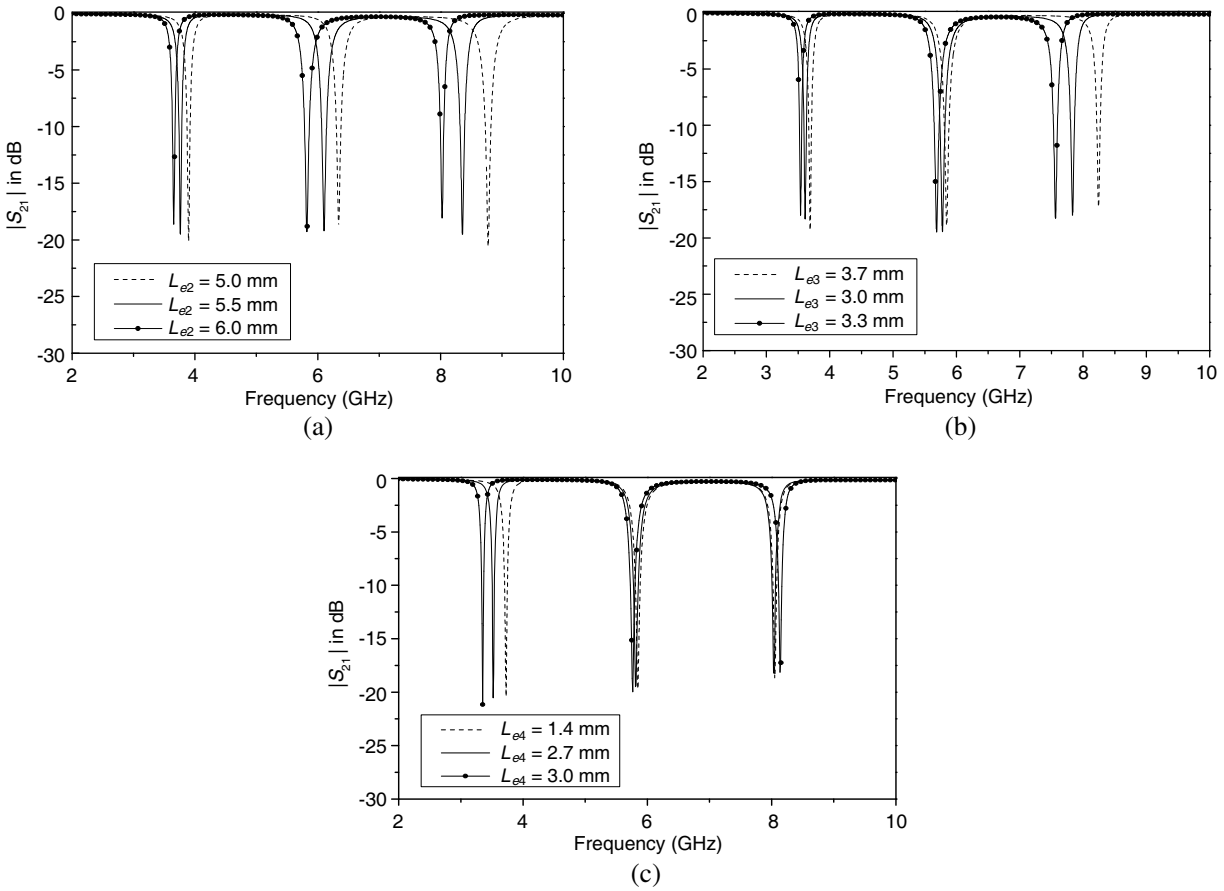

Figure 6. Simulated S-parameters of the coupled triple-mode SIR for various dimensions: (a) L_{e2}, (b) L_{e3}, (c) L_{e4}.

where λ_{notch} is the wavelength of the center frequency of the notched band, f_{notch} the center frequency of the notched band, ε_{eff} the effective dielectric constant, and c the light speed in free space. In addition, the triple-mode SIR dimensions are selected as follows: $w_{e1} = 0.4\,\text{mm}$, $w_{e2} = 0.3\,\text{mm}$, $w_{e3} = 0.4\,\text{mm}$, $w_{e4} = 0.4\,\text{mm}$, $l_{e1} = 6.5\,\text{mm}$, $l_{e2} = 5.5\,\text{mm}$, $l_{e3} = 2.8\,\text{mm}$, $l_{e4} = 3.0\,\text{mm}$, $R = 0.1\,\text{mm}$.

The frequency characteristics of the triple-mode SIR with various dimensions are investigated by HFSS 11.0 to validate the multi-mode resonant property as shown in Fig. 6. It can be seen that the frequency locations of the triple notched bands move down simultaneously as the dimensions of

L_{e2} increases. But only the first notched band increases as L_{e4} decreases, and the third notched band increases as L_{e3} decreases. Therefore, by appropriately adjusting the resonator dimensions, triple notched bands can be achieved at desired frequencies.

4. EXPERIMENTAL RESULTS

The designed UWB BPF is measured with an Agilent N5244A vector network analyzer. Fig. 7 shows the comparison between the simulated and measured results. It can be seen that the fabricated UWB BPF has a pass-band from $3.23 \sim 11.06$ GHz as we expected. Three notched bands with respective 3 dB FBWs of 5.3%, 2.8%, and 3.3% are achieved, which ensure a high selectivity for the designed UWB filter. Inside each notched band, the attenuation is better than -10 dB at the center frequencies of 4.5, 5.9, and 8.0 GHz. The minor discrepancy between simulation and measurement results is mainly due to the reflections from the SMA connectors and the finite substrate. Fig. 8 shows a photograph of the fabricated UWB BPF.

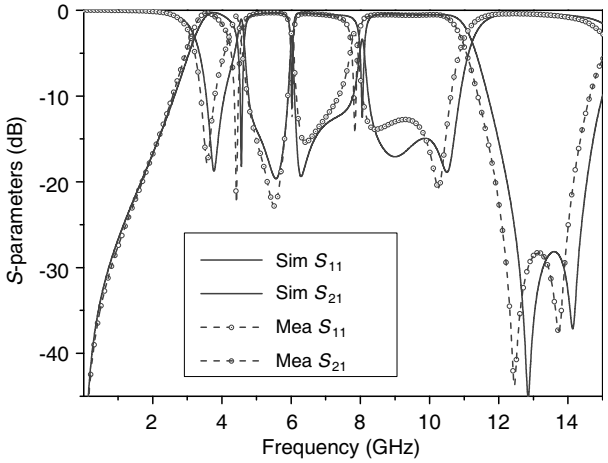

Figure 7. Simulated and measured S-parameters of the designed UWB BPF.

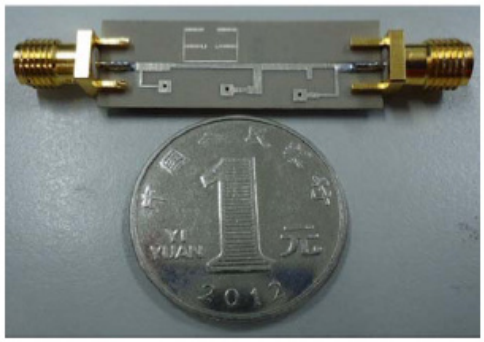

Figure 8. Photograph of the fabricated UWB BPF with triple-notched bands.

5. CONCLUSION

A new microstrip UWB BPF with triple highly rejected notched bands has been proposed and designed in this paper. The basic UWB BPF is efficiently designed by the MGA. Then, triple-notched bands performance is easily generated and realized by controlling the resonance properties of the triple-mode SIR. Good agreement between simulation and measurement results validates the introduced design method. The proposed filter is very useful for modern UWB wireless communication systems due to its distinct properties of simple topology, compact size, and good performance.

ACKNOWLEDGMENT

This work was financially supported by the Science and Technology Project of Guandong province (2013B010401012).

REFERENCES

1. FCC, "Revision of Part 15 of the Commission's rules regarding ultra-wide-band transmission system," Tech. Rep., ET-Docket, 98–153, 2002.

2. Zhu, L., S. Sun, and W. Menzel, "Ultra-wideband (UWB) bandpass filters using multiple-mode resonator," *IEEE Microw. Wireless Compon. Lett.*, Vol. 15, No. 11, 796–798, 2005.
3. Qiang, L., Y.-J. Zhao, Q. Sun, W. Zhao, and B. Liu, "A compact UWB HMSIW bandpass filter based on complementary split-ring resonators," *Progress In Electromagnetics Research C*, Vol. 11, 237–243, 2009.
4. Packiaraj, D., K. J. Vinoy, and A. T. Kalghatgi, "Analysis and design of two layered ultra wide band filter," *Journal of Electromagnetic Waves and Applications*, Vol. 23, Nos. 8–9, 1235–1243, 2009.
5. Wang, H., L. Zhu, and W. Menzel, "Ultra-wideband bandpass filter with hybrid microstrip/CPW structure," *IEEE Microw. Wireless Compon. Lett.*, Vol. 15, No. 12, 844–846, 2005.
6. Shobeyri, M. and M. H. Vadjed-Samiei, "Compact ultra-wideband bandpass filter with defected ground structure," *Progress In Electromagnetics Research Letters*, Vol. 4, 25–31, 2008.
7. Naghshvarian Jahromi, M. and M. Tayarani, "Miniature planar UWB bandpass filters with circular slots in ground," *Progress In Electromagnetics Research Letters*, Vol. 3, 87–93, 2008.
8. Comez-Garcia, R. and J. I. Alonso, "Systematic method for the exact synthesis of ultra-wideband filtering responses using high-pass and low-pass sections," *IEEE Trans. Microw. Theory Tech.*, Vol. 54, No. 10, 3751–3764, 2006.
9. Wong, S. W. and L. Zhu, "Implementation of compact UWB bandpass filter with a notch-band," *IEEE Microw. Wireless Compon. Lett.*, Vol. 18, No. 1, 10–12, 2008.
10. Wei, F., L. Chen, X.-W. Shi, X. H. Wang, and Q. Huang, "Compact UWB bandpass filter with notched band," *Progress In Electromagnetics Research C*, Vol. 4, 121–128, 2008.
11. Wei, F., Q. Y. Wu, X. W. Shi, and L. Chen, "Compact UWB bandpass filter with dual notched bands based on SCRLH resonator," *IEEE Microw. Wireless Compon. Lett.*, Vol. 21, No. 1, 28–30, 2011.
12. Wu, H.-W., M.-H. Weng, and C.-Y. Hung, "Ultra wideband bandpass filter with dual notch bands," *Proc. Asia-Pacific Microwave Conf.*, 33–36, Yokohama, Japan, 2010.
13. Hsiao, P.-Y. and R.-M. Weng, "Compact tri-layer ultra-wideband bandpass filter with dual notch bands," *Progress In Electromagnetics Research*, Vol. 106, 49–60, 2010.
14. Hao, Z.-C., J.-S. Hong, S. K. Alotaibi, J. P. Parry, and D. P. Hand, "Ultra-wideband bandpass filter with multiple notch-bands on multilayer liquid crystal polymer substrate," *IET Microw. Antennas Propag.*, Vol. 3, No. 5, 749–756, 2009.
15. Hao, Z.-C., J.-S. Hong, J. P. Parry, and D. P. Hand, "Ultra-wideband bandpass filter with multiple notch bands using nonuniform periodical slotted ground structure," *IEEE Trans. Microw. Theory Tech.*, Vol. 57, No. 12, 3080–3088, 2009.
16. Luo, X., J.-G. Ma, K. S. Yeo, and E.-P. Li, "Compact ultra-wideband (UWB) bandpass filter with ultra-narrow dual- and quad-notched bands," *IEEE Trans. Microw. Theory Tech.*, Vol. 59, No. 6, 1509–1519, 2011.
17. Nosrati, M. and M. Daneshmand, "Compact microstrip UWB double/single notch-band BPF based on wave's cancellation theory," *IET Microw. Antennas Propag.*, Vol. 6, No. 8, 862–868, 2012.
18. Nosrati, M. and M. Daneshmand, "Developing single-layer ultra-wideband band-pass filter with multiple (triple and quadruple) notches," *IET Microw. Antennas Propag.*, Vol. 7, No. 8, 612–620, 2013.
19. Dong, Y. L., C.-M. Sun, W.-Y. Fu, and W. Shao, "Ultra-wideband bandpass filters with triple and quad frequency notched bands," *Journal of Electromagnetic Waves and Applications*, Vol. 26, Nos. 11–12, 1624–1630, 2012.
20. Hsu, M.-H. and J.-F. Huang, "Annealing algorithm applied in optimum design of 2.4 GHz and 5.2 GHz dual-wideband microstrip line filters," *IEICE Trans. Electronics*, Vol. E88C, No. 1, 47–56, 2005.
21. Zhao, J.-D., J.-P. Wang, G. Zhang, and J.-L. Li, "Compact microstrip UWB bandpass filter with dual notched bands using E-shaped resonator," *IEEE Microw. Wireless Compon. Lett.*, Vol. 23, No. 12, 638–640, 2013.